Real Time Utilization of Extended Kalman Filter Design for Railway Wheelset Dynamics

ISSN (e) 2520-7393
ISSN (p) 2521-5027
Received on 17th Mar, 2018
Revised on 27th Mar, 2018
www.estirj.org

Muhammad Farrukh Shaikh[1], Imtiaz Hussain Kalwar[2], Bharat Lal[3], Tayabuddin Memon[4], Mumtaz Aziz Kazi[3].

[1, 4] Department of Electronic Engineering, Mehran UET, Jamshoro, Pakistan.
[2]Department of Electrical Engineering, DHA Suffa University, Karachi, Pakistan.
[3]Department of Electrical Engineering, ISRA University, Hyderabad, Pakistan.

Email address: muhammadfarrukhshaikh@gmail.com

Abstract: The technique proposed in this paper is to analyze yaw, longitudinal and lateral dynamics for Railway Wheelset Model. As there is a growing need of algorithms to estimate real time non-linear applications. The intricacy and nonlinear nature of the model encounter parameters like orientation, axial velocity, and adhesive forces. To make a real time performance analysis concerned with creeping forces, Extented Kalman Filter (EKF) is involved that linearizes the non- linear behavior of railway wheelset. Furthermore, Creep-Friction characteristics curves are evaluated on MATLAB Simulink to approach the best optimal solution so as to prevent accidents in locomotive applications. The proposed framework justifies implementation with accuracy, cost effectiveness, less complexity and efficient solution for adhesive forces in railway wheelset.

Keywords: *Extended Kalman Filters, Creep forces, Railway Wheelset, Simulink-MATLAB.*

1. Introduction

Adhesion level between railway wheelset is significantly important for secure running of bogie on rails. Low adhesive wear could cause poor traction and braking issues. Usually adhesion smaller than 0.07 (μ>0.07) are of more concern to wheel spin and slip properties of wheelset. These problems lead to risks for passengers like less comfort and damage of wheels and rails. [2]. The braking performance and a good traction also alter with time and weather conditions because for a wet wheelset friction level is much less as compared to dried one. A numerical analysis of friction between rail and wheel is shown in Table 1. Whereas Figure 1 shows traction/slip behavior w.r.t. adhesive conditions. Owing to all circumstances stated above play a substantial role in dynamics of wheel set.

Table.1 Numerical Data of Adhesive Co-efficients.

Description	Adhesive Co-efficient (μ)
Dry	0.560
Wet	0.320
Low	0.072
Very Low	0.038

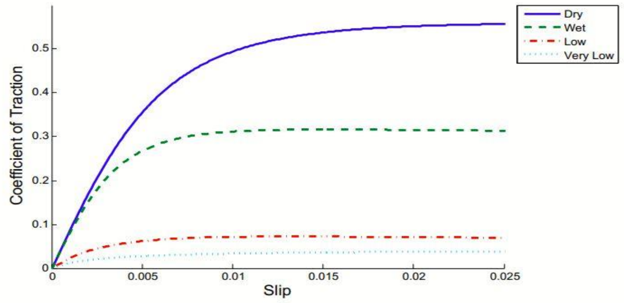

Figure.1. Tractions Condition [3]

Problem: As we are surrounded by many nonlinear and linear systems notifying that for linear systems there are many classical algorithms to optimize but when it comes to nonlinear large scale control systems traditional techniques of linear & dynamic programming completely fail. Since, the research work involves an estimation, prediction and error analysis for wheelset dynamics a predictor-corrector algorithm named Extended Kalman Filter is used. The algorithm is very much efficient for systems with non-linearity. Since, adhesive force is non-linear function of creep forces, mass of vehicle and frictional co-efficient; whereas intolerable creep is produced when applied tractive force exceeds allowable adhesive force during acceleration and deceleration [13].

In this paper a research work is presented to achieve real time information concerned with lateral, longitudinal and yaw dynamics of a railway wheelset through Extended Kalman Filters (EKF). Parameters like inertial measurements, slip, yaw rate are weighed by sensors (accelerometer, gyroscopes & ultrasonic) mounted on wheels and accordingly creep forces are estimated for wheel/rail wear [4].

2. Modelling Railway Wheelset.

To implement Extended Kalman Filter on railway wheelset it is needed to know dynamics of wheelset in terms of all contact forces and their interaction with controlling skidding (slip). Wheelset is a crucial system that has many degree of freedoms (DOFs) it involves mainly normal and tangential contact forces for instance lateral & longitudinal creep forces.

Corresponding author Email address*: muhammadfarrukhshaikh@gmail.com*

2.1 Creeping Forces

Creep is relative movement between rails and wheels in the direction of locomotives. The lateral displacement of wheelset in left and right wheel is givens as follows:

$$\rho_x = \frac{v'_w - v'}{v'} \tag{1}$$

Where v'_w is linear velocity and illustrated by:

$$v'_w = \omega_w r_o \tag{2}$$

Similarly, for right and left wheels

$$v'_{wL} = \omega_{wL}[\, r_o + \gamma(y - y_t)] \tag{3}$$

$$v'_{wR} = \omega_{wR}[\, r_o + \gamma(y - y_t)] \tag{4}$$

Here r_0 is radius of wheel, y_t is the disturbance in lateral direction, γ is conicity of wheel and ω_{wL}/ω_{wR} are angular velocities of left/right wheel. Yaw dynamics cannot be neglected so longitudinal creepages for right and left wheels will be:

$$\rho_{xL} = \frac{r_o\, \omega_{wL} - v}{v} \tag{5}$$

$$\rho_{xR} = \frac{r_o\, \omega_{wR} - v}{v} \tag{6}$$

Whereas Lateral creepages are given as:

$$\rho_{yL} = \frac{y}{v} - \psi \tag{7}$$

$$\rho_{yR} = \frac{y}{v} - \psi \tag{8}$$

Here, ψ is the Yaw Movement. Thus, total creepage is given by:

$$\rho_x = \sqrt{\rho_{xL}{}^2 + \rho_{xR}{}^2} \tag{9}$$

$$\rho_y = \sqrt{\rho_{yL}{}^2 + \rho_{yR}{}^2} \tag{10}$$

Depiction of longitudinal and lateral creep forces for right and left is as follows:

$$F_{iR} = F_R \frac{\rho_{iR}}{\rho_R} \qquad i = x,y \tag{11}$$

$$F_{iL} = F_L \frac{\rho_{iL}}{\rho_L} \qquad i = x,y \tag{12}$$

For cases when slip is very low and co-efficient of friction is significantly high the creep forces can be stated in linear equations.

$$F_{xR} = f_{11}\, \rho_{xR} \tag{13}$$

$$F_{xL} = f_{11}\, \rho_{xL} \tag{14}$$

$$F_{yR} = f_{22}\, \rho_{yR} \tag{15}$$

$$F_{yL} = f_{22}\, \rho_{xl} \tag{16}$$

Whereas declared f_{11} and f_{22} are lateral and longitudinal creepage co-efficients.

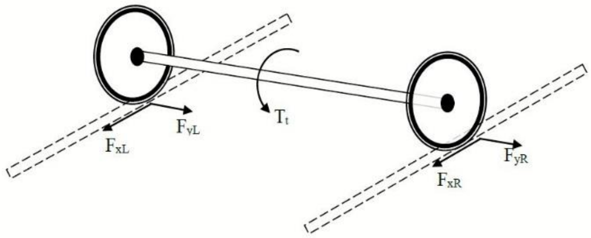

Figure.2. Wheelset Contact Creep Forces.

2.2 Wheel Dynamics.

As discussed above creep forces have essential role in wheelset dynamics. Normally a bogie has two wheelsets and an actuator on each wheelset, placed for proper traction control [5]. The vehicle is linked to the body via springs and dampers in lateral direction. Notify that in Figure 3 dampers and springs are not shown in longitudinal direction whilst they are used for transmitting braking force and traction to chassis of vehicle.

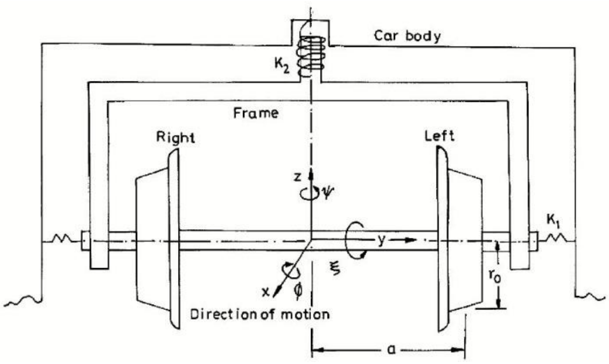

Figure.3. Wheelset co-ordinates and dynamics [6].

In above figure, K_1, K_2 are spring constants, a, r_o are half of track gauge and wheel radius, x, y, z are longitudinal, lateral and vertical displacement & ψ, ϕ, ς are yaw angle, roll angle and rotation angle of wheelset. Yaw motion is affected by longitudinal creep forces whereas lateral motion by lateral creep forces. The paper here is related to three motions i.e. yaw, lateral and longitudinal movements all other motions are neglected. Dynamics of wheelset can further be analyzed by observing Figure 4 that illustrates different situations when wheelset moves on track/rail.

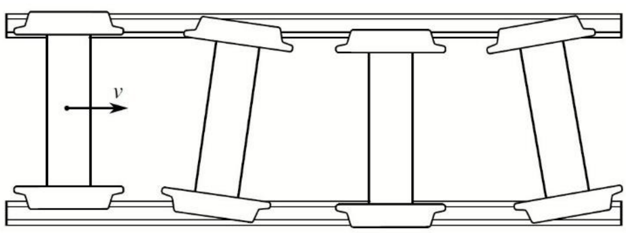

Figure.4. Movements of Wheelset on Rail.

The depicted four movements of railway wheelset and the observed three motions are described below [7] [6].

$y = y'$	$y = 0$	$y = -y'$	$y = 0$
$\varphi = \varphi'$	$\varphi = 0$	$\varphi = -\varphi'$	$\varphi = 0$
$\psi = 0$	$\psi = -\psi'$	$\psi = 0$	$\psi = \psi'$

A kinematic behavior of wheelset oscillations can be easily noticed. Where y', φ', ψ' are amplitudes of oscillations in lateral, yaw and roll directions.

3. Mathematical Calculations.

Since the calculation here involve dynamics of railway wheelset and all factors discussed above are given a shape of matrix equation in this section so as to execute them on MATLAB-Simulink. Extended Kalman Filter (EKF) Estimation here is based on two wheelset models one with large creep forces and other with smaller.

3.1 Wheelset Mathematical Equations.

Longitudinal creep forces on left and right wheels are involved in longitudinal motions

$$M_v = F_{xR} + F_{xL} \tag{17}$$

Although difference between longitudinal creep force affects yaw motion and vice versa for lateral dynamics. Lateral and yaw motions can be describes from equations below

$$m_w\, y = -F_{yR} - F_{yL} + F_c \tag{18}$$

$$I_w\, \psi = F_{xR}L_g - F_xL_g - k_w\, \psi \tag{19}$$

F_c is centrifugal force on round track, I_w is moment of inertia (yaw) and k_w is spring stiffness. Also equations given under for left and right wheel traction T_t is traction torque, T_s is torsional torque & T_L, T_R are tractive torques for left and right wheels.

$$I_R\, \omega_R = T_t - T_s - T_R \tag{20}$$

$$I_L\, \omega_L = T_s - T_L \tag{21}$$

Shaft torsional torque is difference between angular velocities as given below

$$T_s = ks\int(\omega_R - \omega_L)dt + C_s(\omega_R - \omega_L) \tag{22}$$

Where Cs is shaft damping usually ignored being very small. The state variables can be chosen as

$$x = [\, \omega_R \;\; \omega_L \;\; \Theta_S \;\; x' \;\; y \;\; \psi \;\; y' \;\; \psi' \,] \tag{23}$$

where $\Theta_S = \int(\omega_R - \omega_L)dt$ so system based on linear creep forces in equations (13) to (16) can be described as given below [9]:

$$\begin{bmatrix} \omega_R \\ \omega_L \\ \theta_S \\ x' \\ y \\ \psi \\ y' \\ \psi' \end{bmatrix} = \begin{bmatrix} -\frac{r_o^2 f_{11}}{vI_R} & 0 & -\frac{k_s}{I_R} & 0 & \frac{\gamma f_{11}}{I_R} & 0 & 0 & \frac{r_o L_g f_{11}}{vI_w} \\ 0 & -\frac{r_o^2 f_{11}}{vI_L} & \frac{k_s}{I_R} & 0 & -\frac{\gamma f_{11}}{I_R} & 0 & 0 & -\frac{r_o L_g f_{11}}{vI_L} \\ 1 & -1 & 0 & 0 & 0 & 0 & 0 & 0 \\ \frac{r_o f_{11}}{M_v v} & \frac{r_o f_{11}}{M_v v} & 0 & 0 & 0 & 0 & 0 & 0 \\ 0 & 0 & 0 & 0 & 0 & 0 & 1 & 0 \\ 0 & 0 & 0 & 0 & 0 & 0 & 0 & 1 \\ 0 & 0 & 0 & 0 & 0 & \frac{2f_{22}}{m_w} & -\frac{2f_{22}}{m_w} & 0 \\ \frac{r_o L_g f_{11}}{vI_w} & -\frac{r_o L_g f_{11}}{vI_w} & 0 & 0 & -\frac{2L_g \gamma f_{11}}{r_o I_w} & -\frac{k_w}{I_w} & 0 & -\frac{2L_g^2 f_{11}}{vI_w} \end{bmatrix} \begin{bmatrix} \omega_R \\ \omega_L \\ \theta_S \\ x' \\ y \\ \psi \\ y' \\ \psi' \end{bmatrix} + ..$$

$$\begin{bmatrix} \frac{r_o f_{11}}{I_R} \\ \frac{r_0 f_{11}}{I_L} \\ 0 \\ -\frac{2f_{11}}{M_v} \\ 0 \\ 0 \\ 0 \\ 0 \end{bmatrix} + \begin{bmatrix} -\frac{\gamma f_{11}}{I_R} \\ \frac{\gamma f_{11}}{I_L} \\ 0 \\ 0 \\ 0 \\ 0 \\ 0 \\ \frac{2L_g \gamma f_{11}}{r_o I_w} \end{bmatrix} y_t \tag{24}$$

Equation (24) is a mathematical model small signal creep forces the system shown below in equation (29) is second estimation model for large signal creep forces.

$$\Delta F_{xL} = g_{11}\,\Delta\rho_{xL} + g_{12}\,\Delta\rho_{yL} \tag{25}$$

$$\Delta F_{yR} = g_{11}\,\Delta\rho_{xR} + g_{12}\,\Delta\rho_{yR} \tag{26}$$

$$\Delta F_{yR} = g_{21}\,\Delta\rho_{yR} + g_{22}\,\Delta\rho_{yR} \tag{27}$$

$$\Delta F_{yL} = g_{21}\,\Delta\rho_{yL} + g_{22}\,\Delta\rho_{yL} \tag{28}$$

After some calculation state matrix becomes

$$\begin{bmatrix} \Delta\omega_R \\ \Delta\omega_L \\ \Delta\theta_S \\ \Delta x \\ \Delta y \\ \Delta\psi \\ \Delta y' \\ \Delta\psi' \end{bmatrix} = \begin{bmatrix} -\frac{r_o^2 g_{11}}{vI_R} & 0 & -\frac{k_s}{I_R} & 0 & \frac{\gamma g_{11}}{I_R} & \frac{r_0 g_{12}}{I_R} & \frac{r_0 g_{12}}{vI_R} & \frac{r_o L_g g_{11}}{vI_R} \\ 0 & -\frac{r_o^2 g_{11}}{vI_L} & \frac{k_s}{I_L} & 0 & -\frac{\gamma g_{11}}{I_R} & \frac{r_0 g_{12}}{I_L} & -\frac{r_0 g_{12}}{vI_L} & -\frac{r_o L_g g_{11}}{vI_L} \\ 1 & -1 & 0 & 0 & 0 & 0 & 0 & 0 \\ \frac{r_o g_{11}}{M_v v} & \frac{r_o g_{11}}{M_v v} & 0 & 0 & 0 & 0 & \frac{2g_{12}}{M_v v} & -\frac{2g_{12}}{M_v} \\ 0 & 0 & 0 & 0 & 0 & 0 & 1 & 0 \\ 0 & 0 & 0 & 0 & 0 & 0 & 0 & 1 \\ -\frac{r_0 g_{21}}{vm_w} & -\frac{r_0 g_{21}}{vm_w} & 0 & 0 & 0 & \frac{2g_{22}}{m_w} & -\frac{2g_{22}}{m_w} & 0 \\ \frac{r_o L_g g_{11}}{vI_w} & \frac{r_o L_g g_{11}}{vI_w} & 0 & 0 & -\frac{2L_g \gamma g_{11}}{r_o I_w} & -\frac{k_w}{I_w} & 0 & -\frac{2L_g^2 g_{11}}{vI_w} \end{bmatrix} \cdots$$

$$\begin{bmatrix} \Delta\omega_R \\ \Delta\omega_L \\ \Delta\theta_S \\ \Delta x \\ \Delta y \\ \Delta\psi \\ \Delta y' \\ \Delta\psi' \end{bmatrix} + \begin{bmatrix} \frac{1}{I_R} & -\frac{\gamma g_{11}}{I_R} \\ 0 & \frac{\gamma g_{11}}{I_L} \\ 0 & 0 \\ 0 & 0 \\ 0 & 0 \\ 0 & 0 \\ 0 & 0 \\ 0 & \frac{2L_g \gamma g_{11}}{r_o I_w} \end{bmatrix} \begin{bmatrix} \Delta T_m \\ \Delta y_t \end{bmatrix} \tag{29}$$

3.2 Extended Kalman Filter Mathematical Equations.

An advanced version of Kalman Filter predictor- corrector algorithm is Extended Kalman Filter that is widely used in many control engineering applications for evaluation of unmeasured process states. Kalman filters are normally used for linear process estimation whereas Unscented Kalman Filter (UKF) for application with high non-linearity; since we are considering here a wheelset slip with low non linearity therefore using Extended Kalman Filter [12]. The method first linearizes the dynamics with Jacobi method and then predicts states to update them in accordance with actual values. [1][8]. EKF is a probabilistic observer that takes the noise into account during measurement of data from sensors mounted. The algorithm is executed in two steps; firstly, most current states are predicted along with error covariance w.r.t error calculated before. Secondly, correction in predicted states is done if recent calculations are better comparison to actual values then updating of states is done otherwise it remains same [1]. As we cannot use the wheelset dynamics directly to EKF for its non-linear behavior Jacobi method to linearize the system is defined as:

$$F_k = \frac{\partial f}{\partial x}\bigg|_{(\hat{x}_k, u_k, k)} \qquad G_k = \frac{\partial g}{\partial x}\bigg|_{(\hat{x}_k, u_k, k)} \tag{30}$$

The predictor/estimator stage is illustrated by:

$$\hat{x}_k = F_{k-1}\hat{x}_{k-1} + G_{k-1}u_{k-1} + w'_{k-1} \tag{31}$$

$$P'_k = F_{k-1}P'_{k-1}F_{k-1}^T + Q_{k-1} \tag{32}$$

Similarly, corrector step is given by calculating the kalman gain, correcting the prediction and updating covariance as given below via equations.

$$K_k = P'_{k-1}H_k^T(H_k P'_{k-1}H_k^T + R_k)^{-1} \tag{33}$$

$$\hat{x}_k = \hat{x}_{k-1} + K(y_k - H_k\hat{x}_{k-1}) \tag{34}$$

$$P'_k = (I - K_k H_k)P'_{k-1} \tag{35}$$

Where *k* is current state and *k-1* previous state. Table 2 shows description of notations.

Table.2. Description of Notations in EKF.

Description	Notation
$\hat{x}$	State Vector
Y	Output Vector
U	Control Matrix
w'	Predicted Noise Matrix
F	System Matrix
G	Adaptation Matrix
H	Observation Matrix
P	Error Co-variance Matrix
R	Measurement (Sensor) Noise Co-variance.
Q	Noise Co-variance matrix (Process).

It can be observed above that kalman gain in equation (33) weighs the predicted measurements and correspondingly updates current states. In following sections it is shown how the mathematical model estimates system dynamic states via sensor inputs by using MATLAB-Simulink.

4. Simulations and Results.

The simulation here is based on two model estimators to evaluate wheelset rail dynamics because traction conditions change with adhesive co-efficient [10][11]. Simulink based model is shown in Figure 5 the design is executed for two situations maximum adhesion and minimum adhesion w.r.t creep forces. Estimator 1 calculates dynamics at lower creep co-efficients whereas Estimator 2 at higher creep co-efficients.

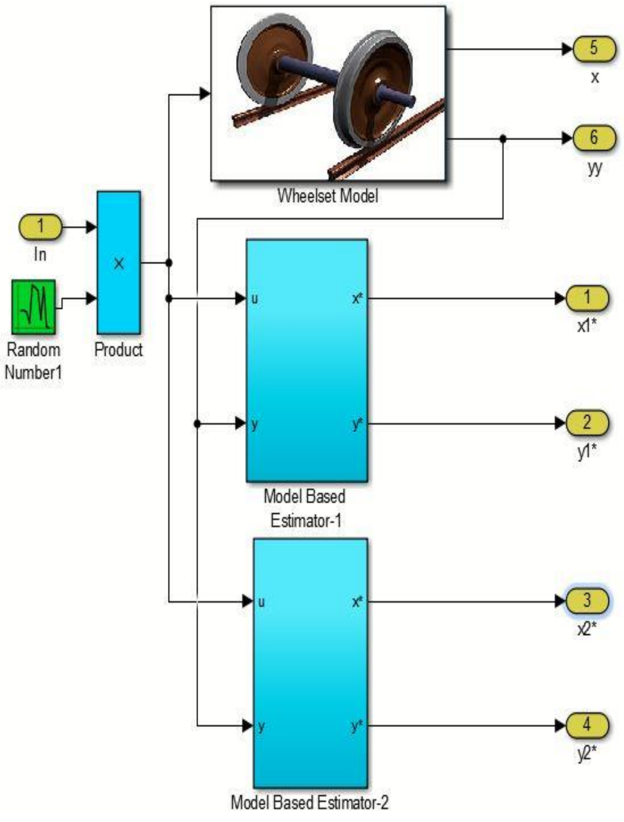

Figure.5. Simulink Model based Estimator.

Also the Simulink model for railways wheelset as per equation (24) is given in Figure.6. The green blocks in design are addition of noise in process (Q) and measurement (R).

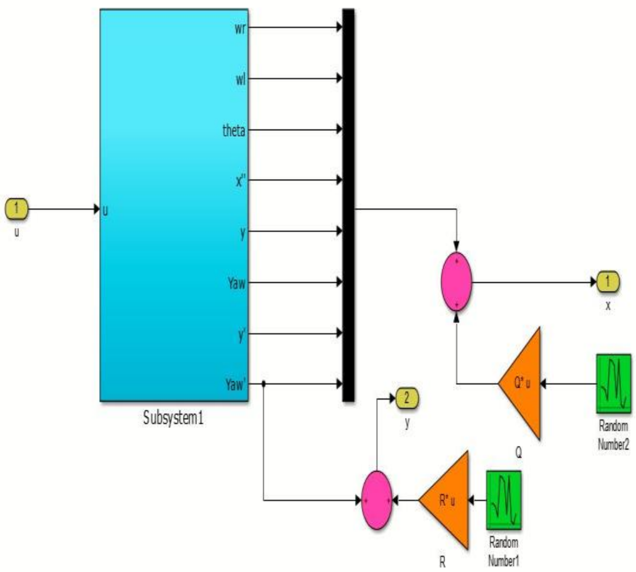

Figure.6. Simulink Model Railway Wheelset.

The simulations results shown below are executed with different creep coefficients for model estimator 1 f_{11}=1E6 and $f_{12}=f_{11}$, on the other hand for model estimator 2 g_{11}=6E6, $g_{22} = g_{11}$, g_{12} = 1.37E6 and $g_{21}= g_{12}$.

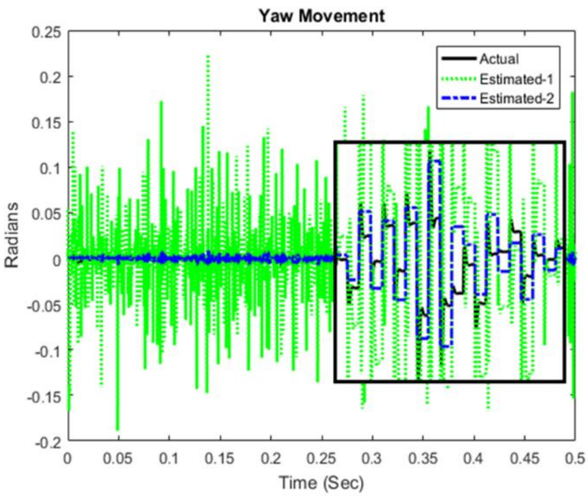

Figure.7. Wheelset Yaw Movement.

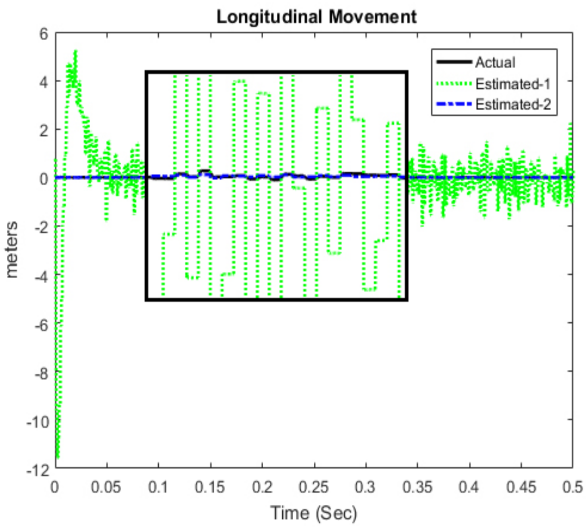

Figure.8. Wheelset Longitudinal Movement.

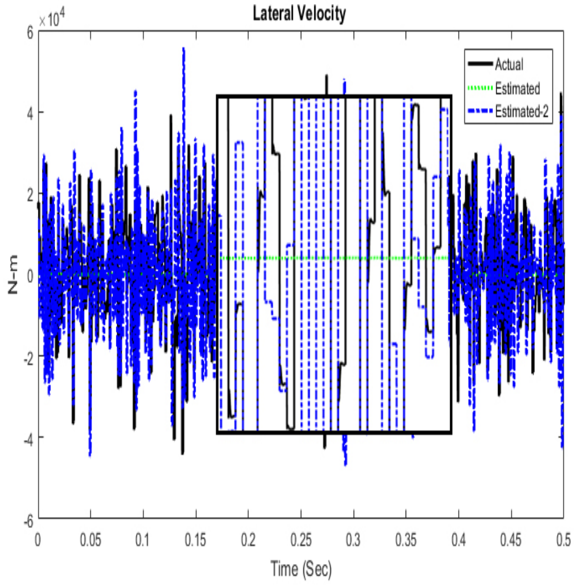

Figure.9. Wheelset Lateral velocity.

It is to notify from above figures 7, 8 and 9 that model 2 gives best estimations of yaw, longitudinal and lateral motions in comparison to model 1. Since, model 2 is tuned on higher creep co-efficient (g_{11}, g_{22}, g_{12} and g_{21}) or at minimum adhesion level thus has greater error as illustrated in Figure 10.

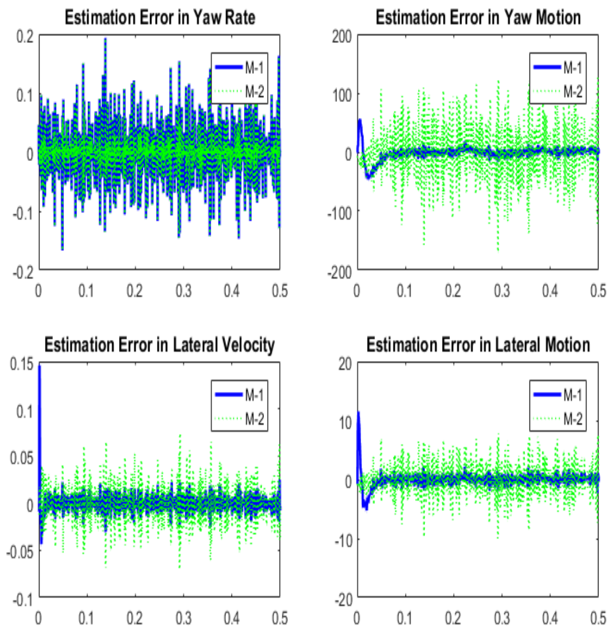

Figure.10. Wheelset Dynamics Error Analysis.

Obviously, we have tuned model 2 with greater creep forces than model 1 so as to examine wheelset dynamics with different traction conditions. The creep forces can be analyzed from Figure 11 which clearly depicts that model 2 has greater longitudinal and lateral creep forces than model 1. In last, it can be stated that for a good traction (adhesion) and wheelset wear, creepage should be maintained at lower rate to avoid any hazardous situation.

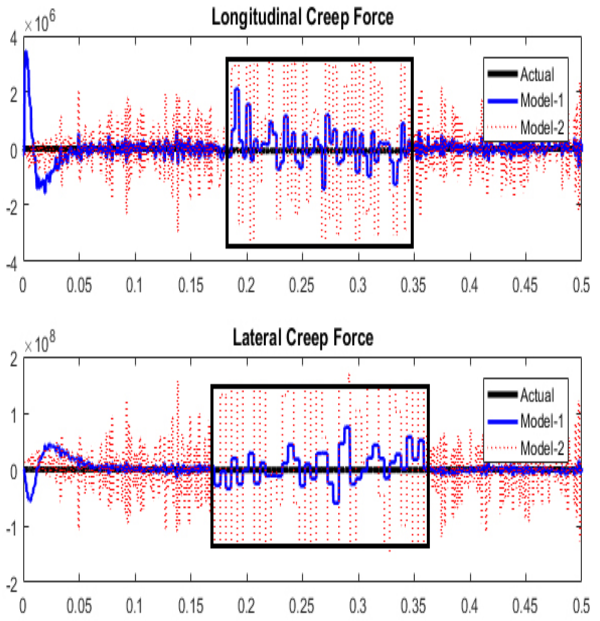

Figure.11. Longitudinal & Lateral Creep Forces.

All simulation results are taken through following parameter values as in Table 3.

Table.3. Parameters Values.

Quantities	Value
Vehicle Mass (M_v)	15000 kg
Forward Velocity (v)	20m/s
Right wheel Inertia (I_R)	134.3 Kgm^2
Left wheel Inertia (I_L)	63.9 Kgm^2
Wheel Radius (r_o)	0.5m
Conicity (γ)	0.15 rad
Wheelset mass (m_w)	1250 Kg
Yaw stiffness (k_w)	2.5E6 N/rad
Torsional stiffness (ks)	6063260 N/m
Curve radius(R_o)	100m
Half Guage(L_g)	0.75m
Wheelset Moment of Inertia(Iw)	700kgm^2

5. Conclusion

The research work presented has successfully estimated three motions i.e. yaw, longitudinal and lateral along with evaluating errors and information concerned to contact creeping forces. Real time prediction of rail wheel contact is essential for continuous traction and preventing hazardous accidental situations. Simulation results, confirm that lower the creepage better will be wheelset assessments regarding actual positions. The work is cost-effective as despite of using expensive and supplementary sensors for measurement, results are simulated by taking into account all necessary environmental parameters. Lastly, proposed work is to be implemented on FPGA for more effective analysis in future.

Acknowledgement

The authors of this paper would like to thank Department of Electronics Engineering Mehran University of Engineering & Technology, Jamshoro, Pakistan for their technical support in providing us Instrumentation & Control Laboratory.

References

[1] M. B. Rhudy, R. A. Salguero and K. Holappa, (2017) "A Kalman Filtering Tutorial For Undergraduate Students", International Journal of Computer Science & Engineering Survey (IJCSES), vol.8, pp. 1-18, 2017.

[2] P.D Hubbard, C. Ward, R. Dixon and R. Goodall, "Models for estimation of creep forces in the wheel/rail contact under varying adhesion levels", International Journal of Vehicle Mechanics and Mobility, vol. 52, pp. 370-386, 2014.

[3] I. Hussain, I. A. Halepoto, W. Kumar, K. Kazi, ”Anti-slip Traction Control of Railway Vehicle Based on Estimated wheel-rail Contact Condition” Sindh Univ. Res. Journal, vol. 45, pp. 373-378, 2013.

[4] C. Peng, X. Gao, L. Wang, Y. Zhang, J. Peng and K. Yang, "Ultrasonic Signal Multiplex Technology for Dynamic Wheelset Defect Detection System", International Conference on Information Technology, Computer Engineering and Management Sciences (ICM), pp.260-262, 2011.

[5] T. X. Mei, and R. M, Goodball, "Practical Strategies for Controlling Railway Wheelsets Independently Rotating Wheels", Journal of Dynamic Systems, Measurement, and Control, vol. 125, pp.354-360, 2003.

[6] Y. Nath and K. Jayadev, "Influence of Yaw Stiffness on the Nonlinear Dynamics of Railway Wheelset", Communication in Nonlinear Science and Numeric Simulation, vol. 10, pp. 179-190, 2005.

[7] M. Antali and G. Stepan, "On the nonlinear kinematic oscillations of railway wheelsets", Journal of Computational and Nonlinear Dynamics, vol. 11, 2016.

[8] P. Pettersson, "Estimation of Vehicle Lateral Velocity", LUP Student Papers, ISSN 0280-5316.

[9] Y. Ji, L. Ren, R. Li and W. Sun, "Study on the Precision of the Guide Control System of Independent Wheel', Journal of Physics: Conference Series, vol.744, pp.1-8, 2016.

[10] I. Hussain and T. X. Mei, "Multi Kalman Filtering Approach for Estimation of Wheel-Rail Contact Conditions", International Conference on Control, pp. 459 -464.

[11] I. Hussain, T. X. Mei and R. T. Ritchings, "Estimation of Wheel-rail Contact Conditions and Adhesion using Multiple Model approach", Journal of Vehicle and Dynamics, vol. 51, pp. 32-53, 2013.

[12] P. Pichik, "Comparison of Different Kalman Filter Types Performance for a Locomotive Slip Control Purposes", Czech Technical University, Prague, May 2017.

[13] C. Uyylan, M. Gokasan, "Extended Kalman Filter Design For Railway Wheelset Traction Motor", Selcuk University Journal of Science and Technology, Vol 5, pp. 432-444, 2017.

About Authors

Engr. Muhammad Farrukh Shaikh is an Electronic Engineer with more than three-year experience in teaching at Undergraduate level. His area of interest includes Control Engineering and Robotics. Currently, he is serving as a Lecturer in the Department of Electrical Engineering at ISRA University Hyderabad, Sindh, Pakistan.

Dr. Imtiaz Hussain Kalwar has research interests that include advanced control and identification and intelligent control systems mainly applied in automotive application. He is currently serving as a Head of Department (HOD) at Department of Electrical Engineering, DHA Suffa University, Karachi, Sindh, Pakistan.

Engr. Bharat Lal is an Electronic Engineer with two years experience in teaching at Undergraduate level. Currently, he is serving as a Lab-Engineer in the Department of Electrical Engineering at ISRA University Hyderabad, Sindh, Pakistan.

Dr. Tayabuddin Memon has research interests in Embedded Systems. He is presently serving as an Associate Professor at Department of Electronic Engineering, Mehran University of Engineering and Technology (MUET), Jamshoro, Sindh, Pakistan.

Engr. Mumtaz Aziz Kazi is professionally an Electrical Engineer with more than seven-year experience in teaching at Postgraduate level. He is serving as a Senior Lecturer in the Department of Electrical Engineering at ISRA University Hyderabad, Sindh, Pakistan.